Biological Journal of the Linnean Society, 2018, **XX**, 1–15. With 3 figures.

Asymmetry drives modularity of the skull in the common dolphin (*Delphinus delphis*)

MORGAN CHURCHILL[1,*], JACOB MIGUEL[2], BRIAN L. BEATTY[2], ANJALI GOSWAMI[3] and JONATHAN H. GEISLER[2]

[1]*Department of Biology, University of Wisconsin Oshkosh, Oshkosh, WI 54901, USA*
[2]*Department of Anatomy, College of Osteopathic Medicine, New York Institute of Technology, Old Westbury, NY 11568, USA*
[3]*Life Sciences Department, Natural History Museum, London SW7 5BD, UK*

Received 6 September 2018; revised 1 November 2018; accepted for publication 2 November 2018

Odontocetes (toothed whales) have amongst the most radically altered skull of any mammal, but no study has tested how these modifications have altered its phenotypic integration. Here, we perform the first rigorous assessment of modularity in *Delphinus delphis*, using a combination of cluster analysis, covariance ratio tests and maximum-likelihood methods, on 27 landmarked skulls. Cluster analysis identified ten semi-autonomous regions (modules), five consisting of bilaterally paired landmarks, while the remaining landmarks were distributed among modules representing the face, zygomatic, nasals, pterygoids and vault. The novel ten-module hypothesis, as well as a simplified version consisting of only the five major modules, was then compared with existing hypotheses formulated for terrestrial mammals based on developmental origin and/or function. We found our novel hypotheses to perform best, except when cranial asymmetry was removed. With the loss of asymmetry, a six-module hypothesis developed for terrestrial mammals was found to best fit the data. Anatomical changes in the skull related to the evolution of echolocation, as well as loss of mastication, best explain the novel modules identified in this study. Our study also provides strong evidence that the evolution of cranial asymmetry is a substantial driver of changes in modularity within whales.

ADDITIONAL KEYWORDS: cranial asymmetry – cranial shape – cranial telescoping – echolocation – EMMLi – mastication – modularity – phenotypic integration – odontocete.

INTRODUCTION

The association and covariation of traits through evolution and ontogeny, as patterned by development and function, is a basic principle of evolutionary biology (Olson & Miller, 1958; Pigliucci & Preston, 2004). These trait associations, or phenotypic integrations, have a significant impact on how different taxa adapt to new environments and lifestyles, shaping the development of novel features and directing changes along preferred trajectories. In recent years, many studies of morphological integration have focused on the mammalian skull (Cheverud, 1995; Goswami, 2006a, b; Mitteroecker & Bookstein, 2008; Drake & Klingenberg, 2010; Shirai & Marroig, 2010; Porto *et al.*, 2013; Santana & Lofgren, 2013; Parr *et al.*, 2016; Machado *et al.*, 2018) with some studies focusing mostly on developmental origin (Drake & Klingenberg, 2010), whereas other studies have used exploratory approaches to identify modules related to function as well (Cheverud, 1982, 1995; Goswami, 2006a, b). Although the exact number of modules and the landmarks associated with specific modules may vary between studies, there is an emerging consensus that six modules can be identified within the therian mammal skull, representing complexes of traits associated with the basicranium, vault, zygomatic-pterygoid, orbit, molars, and the anterior oral and nasals regions (Cheverud, 1995; Goswami, 2006b; Goswami & Finarelli, 2016), although integration is low within some of these modules. These modules all have strong functional correlations. The zygomatic-pterygoid, molars, and anterior oral region and nasals

*Corresponding author. E-mail: churchim@uwosh.edu

are all are related to mastication, while the orbit reflects vision, the vault is associated with the brain, and the basicranium reflects support for the head and attachment to the axial skeleton (Goswami, 2006a).

The above studies have, however, largely focused on terrestrial mammals, although some studies have incorporated pinnipeds (Machado *et al.*, 2018). While the patterns identified appear to hold true for most mammals, clades that have experienced very different adaptive pressures may deviate from the common pattern of modularity, as they also deviate in cranial morphology

One such group are the echolocating whales (Odontoceti). Odontocetes have some of the most radically modified skulls of any living mammal. These modifications include retrograde cranial telescoping (Miller, 1923; Whitmore & Sanders, 1976; Geisler & Sanders, 2003; Churchill *et al.*, 2018), extreme bilateral asymmetry (Ness, 1967; Huggenberger *et al.*, 2017) and simplification of dentition (Werth, 2000; Armfield *et al.*, 2013; Peredo *et al.*, 2018). As a consequence of retrograde cranial telescoping, the frontal and maxillae are greatly expanded in size and contact or nearly contact the supraoccipital, almost completely eliminating the intertemporal region and parietal from dorsal view (Whitmore & Sanders, 1976). Significant overlapping of bones occurs, with the ascending process of the maxillae expanding over the surface of the frontal, and occluding it from view except as a narrow wedge. Furthermore, in most odontocetes, significant differences in the development and position of bones of the face can be detected for the right and left sides of the skull. The midline of the skull is skewed towards the left, with the right premaxilla larger than those on the left (Ness, 1967; Huggenberger *et al.*, 2017). Finally, extant odontocetes generally possess simplified homodont or nearly homodont dentition (Armfield *et al.*, 2013), and a tendency for either increases in tooth count (polydonty; Fordyce, 1982; Armfield *et al.*, 2013), or reductions to or even complete loss of dentition (Werth, 2006; Deméré *et al.*, 2008; Peredo *et al.*, 2018).

Given the bizarre morphology evident in odontocete skulls, different patterns of modularity may be present. However, while the unusual nature of whale cranial morphology has long been recognized (Miller, 1923), only one study has examined modularity in whales, and that study quantified modularity in an ontogenetic series, rather than across adult specimens, and tested only a single model of modularity based on developmental origin of cranial regions (del Castillo *et al.*, 2017). Consideration of alternative models, especially those related to functional structures, is sorely needed, because modifications of the skull observed in odontocetes are almost certainly related to changes in functions of the skull. For instance, unlike terrestrial mammals, odontocetes no longer perform mastication (Hocking *et al.*, 2017), and rather than relying on vision or smell to find prey as do many mammals, odontocetes use echolocation (Au, 1993); this has led to major changes in the facial and narial region related to the production of high-frequency clicks (Heyning & Mead, 1990; Cranford *et al.*, 1996). These changes could have substantially impacted the functional relationships among traits, with commensurate changes in the pattern of cranial modularity.

In this study, we perform the first assessment of modularity within an odontocete taxon, the common dolphin (*Delphinus delphis*, Linnaeus 1758), to determine the impact that cranial telescoping and asymmetry may have had on the phenotypic integration of traits and the overall structure of cranial modularity. With this assessment, we can quantify the level of difference in modularity between terrestrial mammals and an echolocating whale, and estimate the functional constraints that may have influenced the evolution and diversification of odontocetes.

MATERIAL AND METHODS

Sampling

To assess modularity within the dolphin skull, we collected three-dimensional (3D) laser scans of 27 common dolphin skulls present within the mammalogy collections of the American Museum of Natural History (AMNH), a complete list of which is provided in Table 1. All specimens scanned belong to adult individuals, as assessed via a combination of skull size and suture closure. Incomplete and damaged skulls were not scanned or excluded from our sample prior to analyses.

Within our sample set, 11 individuals were male, 13 were female and three were of uncertain sex. Although minor amounts of sexual dimorphism in body size are evident in some *D. delphis* populations, representing up to a 5% difference in body size between adults (Heyning & Perrin, 1994), no evidence of dimorphism in cranial shape has been found (Bell *et al.*, 2002). If some degree of dimorphism does exist in the populations studied here, it is likely to be so minor as to have little influence on the results of the modularity hypotheses being tested.

The majority of the individuals within our analysis (24 individuals) probably belong to *D. delphis bairdi*, Dall 1873, the eastern Pacific long-beaked common dolphin (Committee on Taxonomy, 2017), and were collected from the Pacific coast of Mexico. Two individuals (AMNH 35401 and AMNH 130119) represent individuals belonging to *D. delphis delphis*, the common dolphin, and were collected in New

Table 1. American Museum of Natural History (AMNH) specimens used in this study, with locality and sex information

Locality	Sex	Specimen number(s)
Offshore of Cabo San Lucas, Mexico	Female	AMNH 239125, 239129, 239131, 239134, 239136, 239139, 239140, 239144, 239145, 239146, 239151
Offshore of Cabo San Lucas, Mexico	Male	AMNH 239124, 239126, 239128, 239133, 239135, 239137, 239138, 239141, 239143, 239147, 239148, 239149
Ulster Co., NY, USA	Male	AMNH 130119
New York Co, NY, USA	Unknown	AMNH 35401
Unknown	Unknown	AMNH 176, AMNH 77931

York. A further two *Delphinus* specimens lack specific identity or locality data, and can only be referred to as *D. delphis* ssp. Taxonomy within the genus *Delphinus* remains largely unresolved, and it is possible these two forms represent separate species (Natoli *et al.*, 2006; Cunha *et al.*, 2015; Segura-García *et al.*, 2016); however, for the purpose of this study, and given the overall similarity in morphology, we have treated them as one taxon. Exploratory principal component analysis of landmark data supports this decision, with the Atlantic specimens overlapping in morphospace with those taxa from the North Pacific. All 3D scan data were collected with a Creaform Handyscan 700 laser scanner, with files exported to .ply format at 0.2-mm resolution.

Geometric morphometrics

We placed 67 landmarks on digital models of the skull (Fig. 1), using the program IDAV Landmark (Wiley *et al.*, 2005). Landmarks chosen were modified from those used by Galatius *et al.* (2012), and a description of the landmarks can be found in Supporting Information Appendix S1.

All of the skulls examined possessed obvious cranial asymmetry. To determine the relative impact of cranial asymmetry on modularity, three sets of landmark files were produced. In the first set, the entire skull was landmarked, with no alteration of landmarks. In the second and third sets, landmarks from the right or left side of the skull were removed, leaving those landmarks on the opposite side of the skull and midline intact. These two datasets each contained 39 landmarks per skull. Within the R package 'morpho' (Schlager, 2017) and using the 'mirrofill' function, we then mirrored the bilateral landmarks along an axis defined by six points on the midline of the skull, creating new landmarks based on the positions of existing points on the right or left side of the skull. This mirroring resulted in two new datasets, one based on the left side of the skull, and one based on the right side of the skull, representing complete and now symmetrical skulls containing all 67 landmarks. We produced accurate mirrored images of almost all landmarks used in this study. The exception were landmarks from the tip of the rostrum, which often showed very different and unrealistic orientations when mirrored. This problem with mirroring of the tip of the rostrum was almost entirely due to variable post-mortem drying and separation of the premaxilla during osteological preparation. Due to this issue, we did not mirror these two landmarks and rather maintained the original set of landmarks across all three datasets. All landmark datasets were then subjected to Procrustes superimposition, using the R package 'geomorph' (Adams & Otarola-Castillo, 2013).

Testing models of modularity

We tested whether novel or existing hypotheses of modularity best explain the patterns of correlation of morphological traits using a combination of exploratory (hierarchical cluster analysis; Legendre & Legendre, 1998), confirmatory (CR coefficient; Adams, 2016) and maximum-likelihood approaches (Goswami & Finarelli, 2016). First, we took the 64 landmarks on the dolphin skull and assigned them into modules defined from five existing hypotheses of cranial modularity (Appendix S1). All but one of these models (the three-module hypothesis of del Castillo *et al.*, 2017) are derived from analyses of modularity of terrestrial mammalian skulls, and in some cases use very different landmarks from those typically used in morphometric analysis of cetacean skulls (antorbital notch, etc). When a given landmark on the dolphin skull did not align with existing landmarks within these module hypotheses, we approximated what module they would belong to on the basis of the regions of the skull and bones they were associated with, and where those points would exist on a terrestrial mammal skull. Known module hypotheses selected for use in this study include: the two-module hypothesis of Drake & Klingenberg (2010), where landmarks are segregated into a facial or neurocranial region; the three-module hypothesis of del Castillo *et al.* (2017), where landmarks are sorted into three modules on the basis of developmental origin (rostrum, neurocranium and basicranium); the six-module hypothesis of Cheverud (1995), which sorts cranial landmarks into

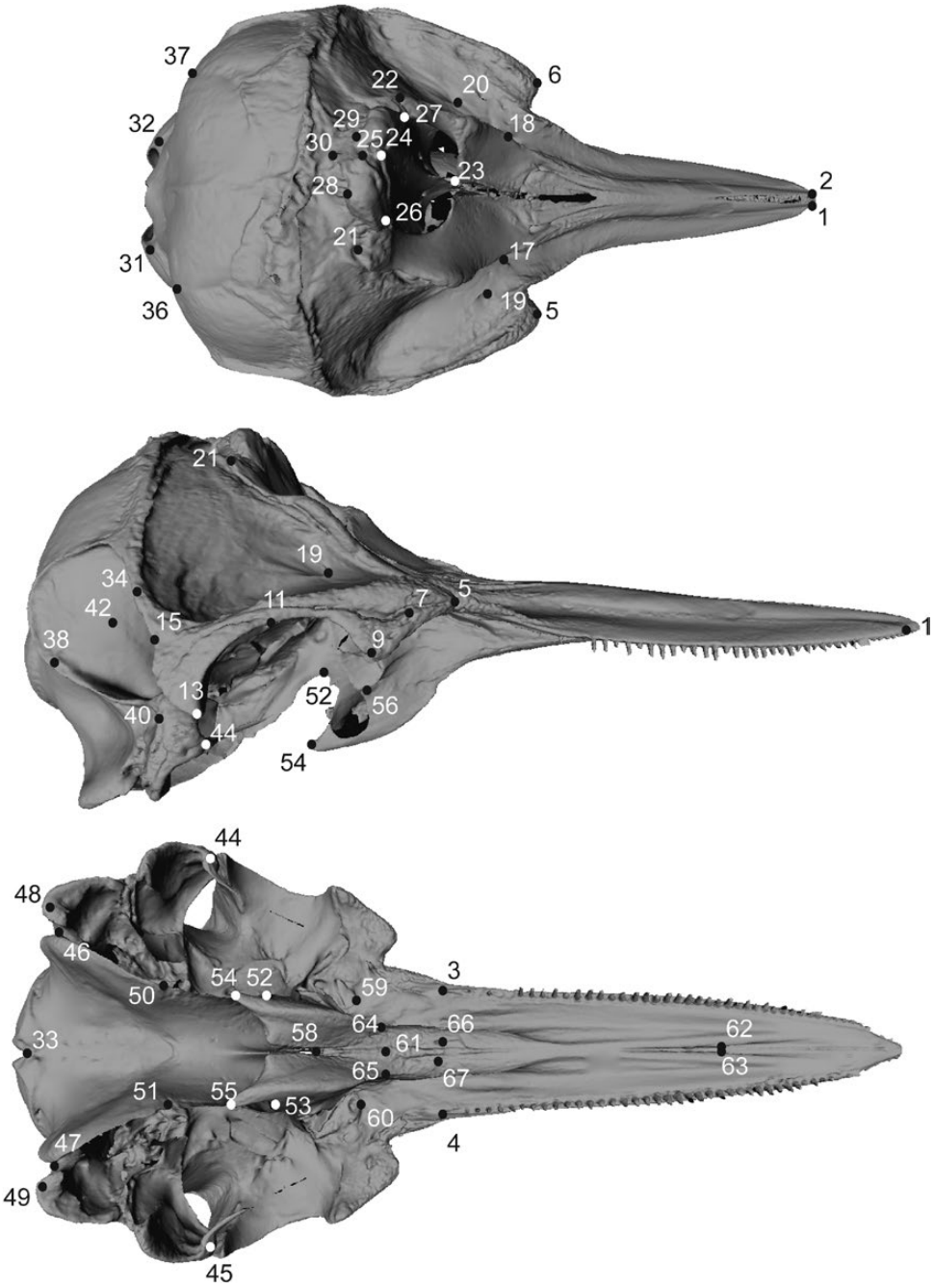

Figure 1. Cranial landmarks in posterodorsal (top), lateral (middle) and ventral (bottom) view on the skull of *Delphinus delphis* (AMNH 239149). Landmarks are listed and described in Appendix S1.

modules on the basis of a combination of functional and developmental relationships (oral, nasal, orbit, vault, zygomatic and base); the six-module hypothesis of Goswami (2006a), which divides the skull into anterior oral-nasal, molar-palatal, orbit, zygomatic-pterygoid, vault and basicranial regions; and finally an eight-module hypothesis, based on the ten-module hypothesis of Parr *et al.* (2016), which divides the skull into regions associated with the distal snout and palatine, the proximal palatine and anterior braincase, the proximal snout, the olfactory, the basicranium and occipital condyles, the zygomatic and temporal-mandibular joint (TMJ), and the anterior basicranium. For the last of these hypotheses, we used eight modules rather than ten, as the original hypothesis segregated the zygomatic and TMJ into three regions with bilateral

asymmetry: the left zygomatic arch and left TMJ; the right TMJ; and the right zygomatic arch. As some of our analyses explicitly remove asymmetry of the skull, we concluded that merging these modules into one module would be more appropriate for our study.

Although the above hypotheses cover a broad range of possible models for cranial organization, they were not tailored to take into account either cranial telescoping or asymmetry (other than the amendment noted above), nor were they implemented using landmarks typically used in cetacean morphometric analysis (e.g. Galatius *et al.*, 2012; Galatius & Goodall, 2016; del Castillo *et al.*, 2017). Because of this, we cannot fully exclude the existence of unique patterns of phenotypic variation in the skull that might best represent odontocete cranial variation. To test whether novel cranial modules exist for odontocetes, we carried out exploratory approaches using hierarchical cluster analysis. The interpretation of cranial modules derived from cluster analysis should be viewed cautiously; some datasets may have low co-phenetic variation (Zelditch *et al.*, 2009), and by default a cluster analysis will always find clusters, even if there is poor structure in the dataset (Goswami & Polly, 2010). However, as an exploratory method it allows the assessment of correlations between landmarks without a priori assignment of landmarks to modules.

To perform the cluster analysis, covariance matrices produced as a consequence of our Procrustes superimposition were then converted to landmark distance correlation matrices via the R package 'paleomorph'. These distance matrices were then used to produce hierarchical cluster plots using Wards linkage method in the R package 'pvclust' (Suzuki & Shimodaira, 2006), with *P* values assigned to each cluster. The least inclusive clusters with $P \leq 0.05$ were used to define modules; landmarks which were not found to cluster with any other group of landmarks were left unassigned to a module. The modules identified in analyses of the whole skull, the right mirrored skull and the left side mirrored skulls were used to define new hypotheses of phenotypic modularity to be tested alongside the five prior hypotheses (Appendix S1).

After assignment of landmarks to modules, we then tested the degree of modularity in the hypothetical modules using the covariance ratio (CR) coefficient (Adams, 2016). CR is a measure of the pairwise covariance of landmarks between and within modules, and the CR modularity test compares this value with that expected if landmarks were randomly assigned to different modules. Thus, significant *P* values ($P \leq 0.05$) indicate a higher degree of integration within modules than expected from chance alone. CR coefficients were generated for all three datasets and all hypotheses (existing and novel) using the modularity.test function in 'geomorph' (Adams & Otarola-Castillo, 2013).

While the CR coefficient is a useful tool to assess hypotheses of modularity, it can only confirm if hypotheses are significantly different from a null hypothesis of random distribution. CR coefficients are incapable of determining, if multiple hypotheses are significant, which individual hypothesis best fits the data. To determine which hypothesis best fit the data, we used a maximum-likelihood approach with model parameterization, using the R package 'EMMLi' (Goswami & Finarelli, 2016). EMMLi uses maximum likelihood and Akaike's information criterion (AIC) to examine and compare different trait correlation matrices with different levels of complexity. Not only does this allow us to determine which proposed module hypothesis best fits the data, but we can also vary model parameters that influence integration between and within modules. Models examined for this test included a hypothesis of no modularity in the dataset, as well as the existing and novel hypotheses tested above. For the existing and novel hypotheses, we varied the correlation coefficient (ρ; Table 2), by using the same ρ for within and between modules, separate ρ for within and between modules, the same ρ for within modules but different ρ between modules, and different ρ for within modules but the same ρ for between modules, following Goswami & Finarelli (2016). Overall, we tested 31 models with two to 57 parameters, depending on the number of assigned modules and the number of parameters varied.

RESULTS

Cluster analysis and identification of novel modules

Cluster analysis of the entire skull, unaltered by mirroring, resulted in the recovery of ten distinct modules (Fig. 2). The same clusters are identified when asymmetry is removed from the landmarks and either the left or the right side is mirrored. Clusters that were significantly supported correspond to the following regions: face, consisting of landmarks associated with the lacrimal, the antorbital process of the frontal, the anterior infraorbital foramen, the posterior portion of the premaxilla, and the nasal septum; zygomatic, consisting of landmarks associated with the postorbital process of the frontal, the zygomatic process of the squamosal, the paraoccipital and the palatine–maxilla suture; nasals, consisting of landmarks associated with the nasals and the intersection of the parietal/interparietal and frontal; pterygoids, consisting of landmarks associated with the posterior palatine, pterygoid hamuli and Eustachian notch; the anterior tip of the pterygoids; vault, consisting of landmarks associated with the occipital; the posteriormost

Table 2. Model descriptions and parameters, for all 43 models used in EMMLi model selection analysis

Model ID	Base model structure	Number of modules	Model description	Number of parameters
1	No modules	0	One ρ for all correlations	2
2A	Drake & Klingenberg (2010)	2	Same ρ for within and between modules	3
2B	Drake & Klingenberg (2010)	2	Separate ρ for within and between modules	4
3A	del Castillo *et al.* (2017)	3	Same ρ for within and between modules	3
3B	del Castillo *et al.* (2017)	3	Same ρ for within modules but separate ρ between modules	5
3C	del Castillo *et al.* (2017)	3	Separate ρ for within modules but same between modules ρ	5
3D	del Castillo *et al.* (2017)	3	Separate ρ for within and between modules	7
4A	Cheverud (1995)	6	Same ρ for within and between modules	3
4B	Cheverud (1995)	6	Same ρ for within modules but separate ρ between modules	17
4C	Cheverud (1995)	6	Separate ρ for within modules but same between modules ρ	8
4D	Cheverud (1995)	6	Separate ρ for within and between modules	22
5A	Goswami (2006a)	6	Same ρ for within and between modules	3
5B	Goswami (2006a)	6	Same ρ for within modules but separate ρ between modules	17
5C	Goswami (2006a)	6	Separate ρ for within modules but same between modules ρ	8
5D	Goswami (2006a)	6	Separate ρ for within and between modules	22
6A	Parr *et al.* (2016_	7	Same ρ for within and between modules	3
6B	Parr *et al.* (2016)	7	Same ρ for within modules but separate ρ between modules	23
6C	Parr *et al.* (2016)	7	Separate ρ for within modules but same between modules ρ	9
6D	Parr *et al.* (2016)	7	Separate ρ for within and between modules	29
7A	Novel ten-module	10 + unintegrated	Same ρ for within and between modules	4
7B	Novel ten-module	10 + unintegrated	Same ρ for within and between modules, separate ρ for unintegrated	3
7C	Novel ten-module	10 + unintegrated	Same ρ for within modules but separate ρ between modules	48
7D	Novel ten-module	10 + unintegrated	Separate ρ for within modules but same between modules ρ	13
7E	Novel ten-module	10 + unintegrated	Separate ρ for within modules but same between modules ρ, separate ρ for unintegrated	12
7F	Novel ten-module	10 + unintegrated	Separate ρ for within and between modules	57

Table 2. Continued

Model ID	Base model structure	Number of modules	Model description	Number of parameters
8A	Novel five-module	5 + unintegrated	Same ρ for within and between modules	4
8B	Novel five-module	5 + unintegrated	Same ρ for within and between modules, separate ρ for unintegrated	3
8C	Novel five-module	5 + unintegrated	Same ρ for within modules but separate ρ between modules	13
8D	Novel five-module	5 + unintegrated	Separate ρ for within modules but same between modules ρ	8
8E	Novel five-module	5 + unintegrated	Separate ρ for within modules but same between modules ρ, separate ρ for unintegrated	7
8F	Novel five-module	5 + unintegrated	Separate ρ for within and between modules	17

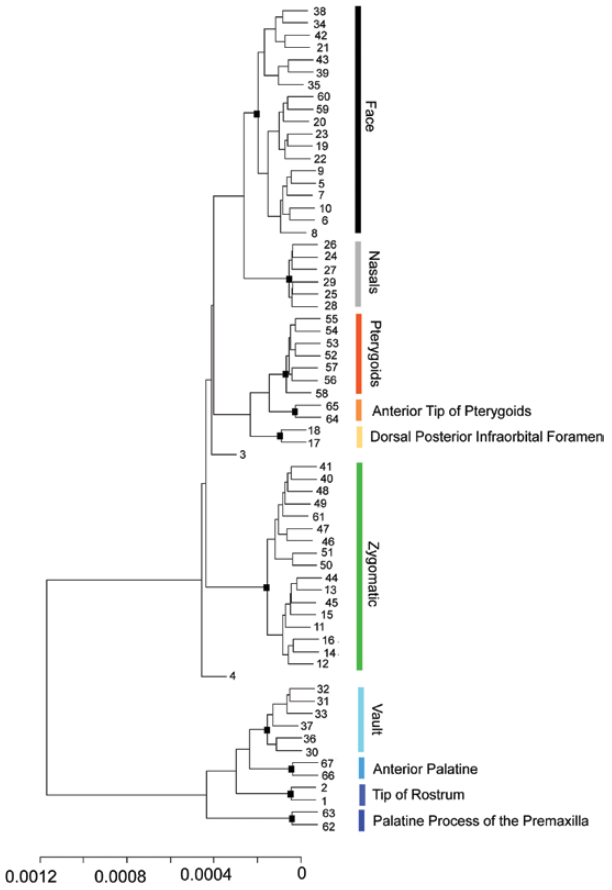

Figure 2. Hierarchal Euclidean cluster analysis of cranial landmarks for *Delphinus delphis*, based on the complete skull. Clusters indicated by black boxes have a *P* value ≤0.05. The ten modules indicated are named on the right. Results of cluster analysis for left and right mirrored skulls are identical.

infraorbital foramina; the anterior palatine; the tip of rostrum; and the palatine process of the premaxilla. Of all the landmarks incorporated, only one set of bilateral landmarks did not clearly form a significant cluster with any other landmark including each other: the distal alveoli of the upper tooth row.

However, at least five of these modules are represented by bilateral landmarks, and are not clearly associated with any other set of landmarks. These included the tip of the rostrum, the dorsal posterior infraorbital foramina, palatine process of the premaxilla, anterior tip of the pterygoid and anterior tip of the palatine. To avoid having a novel hypothesis so heavily weighted towards single landmarks, we also tested a condensed version of the ten-module hypothesis in which the above points were not assigned to any specific module, resulting in a new five-module hypothesis.

Modularity tests

CR tests found varying significant support for the different hypotheses, on both asymmetrical and mirrored skulls (Table 3). The three-module (del Castillo *et al.*, 2017), six-module [both Cheverud (1995) and Goswami (2006a)] and novel five- and ten-module hypotheses were supported ($P \leq 0.05$) for all three datasets. The two-module hypothesis (Drake & Klingenberg, 2010) was only significant when the right side of the skull was mirrored, while the eight-module hypothesis (Parr *et al.*, 2016) was significant only for the asymmetrical skull.

EMMLI analysis also showed that model fit varied with the dataset being used (Table 4; Appendix S2). For the unaltered asymmetrical skull, the most complex model (varying ρ for within and between models) of

Table 3. Results of modularity tests implemented through the Geomorph package in R

Module hypothesis	Entire skull	Entire skull, left side mirrored	Entire skull, right side mirrored
Drake & Klingenberg (2010) (two-module)	CR = 0.87 *P* = 0.11	CR = 1.03 *P* = 0.13	**CR = 1.01** ***P* = 0.001**
del Castillo *et al*. (2017) (three-module)	**CR = 0.82** ***P* = 0.02**	**CR = 1.03** ***P* = 0.002**	**CR = 1.02** ***P* = 0.002**
Cheverud (1995) (six-module)	**CR = 0.73** ***P* = 0.03**	**CR = 1.05** ***P* = 0.001**	**CR = 1.04** ***P* = 0.001**
Goswami (2006a) (six-module)	**CR = 0.70** ***P* = 0.001**	**CR = 1.07** ***P* = 0.01**	**CR = 1.07** ***P* = 0.05**
Parr *et al.* (2016) (eight module)	**CR = 0.70** ***P* = 0.001**	CR = 1.11 *P* = 0.22	CR = 1.09 *P* = 0.09
Novel ten-module	**CR = 0.57** ***P* = 0.001**	**CR = 1.22** ***P* = 0.01**	**CR = 1.22** ***P* = 0.07**
Novel five-module	CR = 0.84 *P* = 0.21	CR = 1.57 *P* = 0.32	CR = 1.70 *P* = 0.932

CR, covariance ratio. Statistically significant results are in bold type.

Table 4. Results of EMMLi model selection analyses on five landmark datasets

Model ID	Log likelihood	Number of parameters	AIC_C	ΔAIC_C	Model log likelihood	Model posterior probability
Entire skull						
7F	**3234.74**	**57**	**−6352.4**	**0**	**1**	**1**
7D	3171.65	13	−6317.13	35.28	2.19E-08	2.19E-08
7E	3168.56	12	−6312.97	39.43	2.74E-09	2.74E-09
8F	3120.02	17	−6205.77	146.63	1.44E-32	1.44E-32
8D	3110.25	8	−6204.43	147.97	7.38E-33	7.38E-33
Entire skull, left side of cranium mirrored						
4D	**−1940.51**	**22**	**3925.48**	**0**	**1**	**1**
7F	−2168.88	57	4456.83	531.35	4.17E-116	4.17E-116
4B	−2231.88	17	4498.03	572.55	4.71E-125	4.71E-125
8F	−2504.04	17	5042.36	1116.87	2.98E-243	2.98E-243
4C	−2601.36	8	5311.53	1386.07	1.04E-301	1.04E-301
Entire skull, right side of cranium mirrored						
4D	**−1423.02**	**22**	**2890.5**	**0**	**1**	**1**
7F	−1618.63	57	3354.34	463.84	1.90E-101	1.90E-101
4B	−1814.28	17	3662.84	772.34	1.94E-168	1.94E-168
6D	−1830.08	29	3718.95	828.45	1.27E-180	1.27E-180
8F	−1905.89	17	3846.06	955.56	3.19E-208	3.19E-208

Only the top five models out of 44 are shown for each dataset. The single best model is indicated in bold type, and Model IDs are listed in Table 2. For full results, please see Appendix S2.

the novel ten-module hypothesis was found to best fit the data. Variations of this model or the five-module hypothesis all had the lowest corrected AIC (AIC_C) scores and best fitted the data.

When either the left or the right side of the skull was mirrored, the most complex model of the six-module (Cheverud, 1995) hypothesis was always recovered as best fitting the data. When the left side of the skull was mirrored, variations of this hypothesis, as well as the novel ten- and five-module hypotheses, also had particularly low AIC_C scores. When the right side was mirrored, variations of the Parr *et al.* (2016) eight-module hypothesis, as well as novel module hypotheses, all had low AIC_C scores.

DISCUSSION

CHANGES IN FEEDING APPARATUS AND CRANIAL MODULARITY

The dolphin skull is extremely modified when compared to most terrestrial mammal skulls, which has substantially altered the modularity of the skull. These modifications are the result of adaptations to an aquatic lifestyle, and include the loss of mastication and specializations towards raptorial and suction feeding (Werth, 2000; Hocking *et al.*, 2017), development of echolocation to navigate underwater (Au, 1993) and streamlining of the body for high-speed aquatic locomotion (Fish & Hui, 1991; Cozzi *et al.*, 2017). Below we discuss the specific modules recovered for the *Delphinus* skull (Fig. 3), and how they may

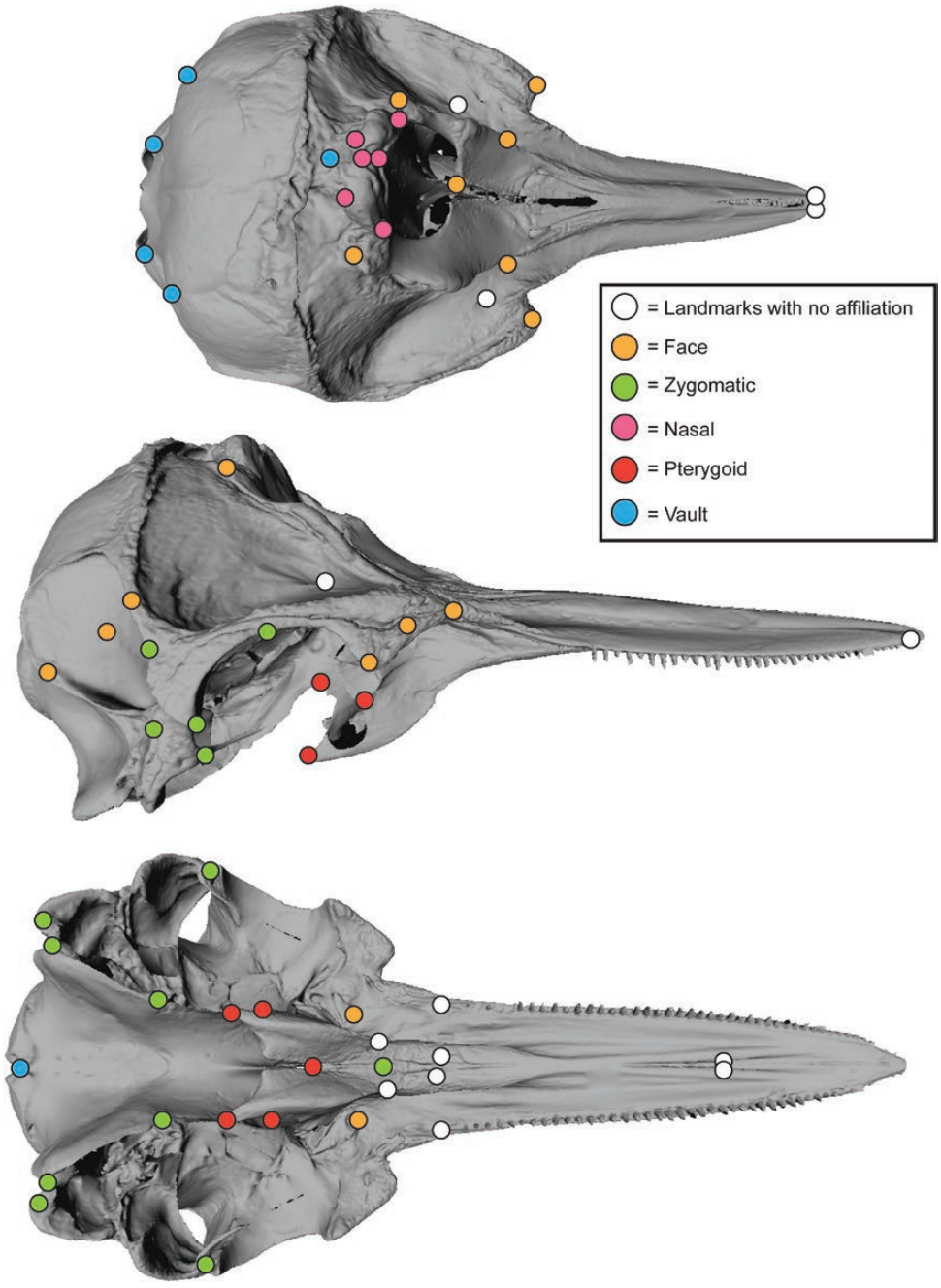

Figure 3. Cranial landmarks with module association in posterodorsal (top), lateral (middle) and ventral (bottom) view on the skull of *Delphinus delphis* (AMNH 239149).

reflect the above adaptations. For the purpose of this discussion, we will only focus on the more complex module hypotheses presented by Cheverud (1995), Goswami (2006a) and Parr *et al.* (2016). The two- and three-module hypotheses of Drake & Klingenberg (2010) and del Castillo *et al.* (2017) were generally not supported in the EMMLi analyses as being the best fits to the data. In addition, they are largely based on development origins, not function, and thus do not translate as well for a discussion focused on aquatic adaptations.

One substantial change associated with adaptations to an aquatic lifestyle are changes in the feeding apparatus, as a result of changes in prey capture, manipulation and processing (Hocking *et al.*, 2017; Kienle *et al.*, 2017). Although detailed studies of feeding mode are absent for *Delphinus*, it is probably a ram feeder, much like its close relative *Tursiops* (Bloodworth & Marshall, 2005). After prey are captured, they are swallowed whole, with no mastication. Adaptations towards ram feeding and loss of mastication have resulted in the development of a polydont and homodont dentition situated in a long, narrow rostrum (Armfield *et al.*, 2013).

Changes in the above features have probably impacted the modularity of the skull in several ways. First, significant rostral elongation in *Delphinus* has resulted in isolation by distance of one bilateral pair of landmarks, the tips of the premaxillae, from all the other landmarks. Thus, it is not surprising that this pair of landmarks is recovered as its own unique module, and cannot be associated with any other module. Previous modularity studies on terrestrial mammals have placed similar landmarks with the oral (Cheverud, 1995), anterior oral-nasal (Goswami, 2006a) or distal snout (Parr *et al.*, 2016) modules. Polydonty and homodonty of the dentition, as well as variation in dental count, prevented us from locating some traditional mammalian cranial landmarks that rely on tooth locus (e.g. landmarks relative to canines and molars). In extant cetaceans there are few unambiguous, homologous features on the skull between the tip of the rostrum and the face to provide additional landmarks. These landmarks, if they existed, could help to associate rostral landmarks with other modules. Other potential landmarks along the rostrum seem variable and difficult to place; for instance, posterior terminus of the palatine process of the premaxilla can often be hard to identify in 3D scans of *Delphinus* skulls, due to the difficulty in distinguishing this suture on the scans available to us.

Because of homodont and polydont dentition, as well as variation in tooth count and development within the species, we only applied one dentition-related landmark, position of the distal tooth alveolus. This is in contrast to other modularity studies, which have employed five (Goswami, 2006a) or 14 (Parr *et al.*, 2016) landmarks related to dentition. It is perhaps not surprising then that our study was unable to confidently place this pair of landmarks with any other modules, much like the landmarks at the tip of the snout. Goswami (2006a) found a distinct molar module which also includes the palatine and jugal; we do not find such an association. The lack of significant unambiguous landmarks associated with the dentition of whales makes it difficult to test the role of mastication in modularity within whales. Dolphins do not use their teeth in chewing, and the upper dentition of odontocetes mostly functions in piercing and holding prey, rather than physically breaking down food items (Hocking *et al.*, 2017). If mastication is no longer a constraint on skull shape, we might see both loss of landmarks in the relevant area of the skull along with loss of modularity, and untangling these influences is not easy. Further work, using surface landmarks rather than fixed points, is needed to test the impact of loss of mastication on modularity.

Loss of mastication not only influences dentition, but may influence the palate as well, severing the link between the teeth and palate. The loss of these functional constraints may also explain our failure to recover the anterior tip of the palatine as belonging to any other module of the skull, although this landmark was also difficult to identify in many specimens, due to obliteration of the suture between the palatine and maxilla in some specimens.

Evolution of echolocation and changes in cranial modularity

Another major adaptation for an aquatic lifestyle seen in odontocetes is the use of echolocation for underwater navigation, which uses the echoes from the whale's own vocalizations to produce accurate sonar maps of the environment (Au, 1993). During echolocation, high-frequency sound is produced by a forcing air through and adjacent to a pair of structures in the nasal passages called the monkey lips/dorsal bursae complex (MLDB), or phonic lips (Cranford *et al.*, 1996, 2011). As air passes through these structures, they cause vibrations in a set of fat-filled sacs referred to as the anterior and dorsal bursae; these vibrations are then passed into a large and fat-filled melon (Cranford *et al.*, 2014). The melon focuses and emits these sounds forward through the water (Mckenna *et al.*, 2011). As a consequence of this radical modification of facial soft anatomy, muscles formerly associated with facial expression have been completely lost or heavily modified (Mead, 1975), with most of the facial musculature now devoted to sound production and focusing, as well as to respiration (Cozzi *et al.*, 2017).

Adaptations towards underwater sound production may thus drive the apparent 'split' of the orbit module (*sensu* Cheverud, 1995; Goswami, 2006a) into two distinct modules: face and zygomatic. The face consists of features of the skull associated with the facial fossa, the antorbital region, the lateral portion of the external nares, the anterior infraorbital foramen and the parietals. Numerous nasofacial muscles (nasal plug muscle, pars anterointernus, etc.) associated with the nasal complex originate in this area (Mead, 1975; Heyning, 1989; Heyning & Mead, 1990; Cozzi *et al.*, 2017). Landmarks associated with the parietal on the lateral side of the skull (e.g. junction of the exoccipital, parietal and squamosal bones; dorsal point of the squamosal) are also associated with this module. This rearrangement may be a result of cranial telescoping placing the face into a more posterior position (Churchill *et al.*, 2018), constraining and influencing the size of the temporal fossa.

Also related to echolocation is the pterygoid module. In typical terrestrial mammals, the pterygoids are relatively small, but in odontocetes they form prominent yet delicate structures that make up the medial and lateral walls of the pterygoid sinus (Rommel *et al.*, 2006). These sinuses are part of a much larger and more complex air sac system unique to whales (Racicot & Berta, 2013) that reaches its greatest morphological diversity within odontocetes (Fraser & Purves, 1960). This sinus system may function in both the reflection of sound produced during echolocation (Norris, 1964; Racicot & Berta, 2013), as well as to acoustically isolate the sound-generating and sound-conducting regions of the skull (Cranford *et al.*, 2008a, b; Racicot & Berta, 2013). The importance of the pterygoid bones in constraining the shape and size of the pterygoid sinus is likely to play a role in these landmarks forming their own module, in contrast to previous studies on terrestrial mammals where these landmarks are linked with the basion (Cheverud, 1995), the zygomatic (Goswami, 2006a), or various other modules associated with the ventral surface of the skull (Parr *et al.*, 2016). Whether this module association evolved with echolocation in odontocetes, or evolved alongside underwater hearing, requires further testing of archaeocete and mysticete whales.

As demonstrated above, the development of echolocation seemingly had a major influence on the modularity of the skull. Echolocation in odontocetes has replaced vision as the most important sense used in navigation, to the extent that some taxa, such as the Ganges and Indus River dolphins *Platanista*, are nearly blind, resulting in reduced importance of a single integrated orbit module. However, modularity being influenced by the evolution of echolocation has not been found for other groups of mammals, with bats showing no major shift in modularity as a result of specialization towards echolocation (Santana & Lofgren, 2013). Differences in the influence of echolocation on modularity between these two groups is probably a result of differences in the underlying anatomy used by the two clades of mammals. While odontocetes exhibit substantial modification of the skull related to the production of sound used in echolocation, bats show relatively minor changes in the nasal cavity, and otherwise have typical mammalian skulls. At least some of these differences may be due to the additional adaptations that whales required to hear underwater, preceding the evolution of echolocation, adaptations that bats did not require.

With the split of the orbit module into two new modules, the postorbital process of the frontal is now linked with the zygomatic process of the squamosal, which it nearly contacts. The postorbital process of the frontal forms part of the zygomatic arch (Fordyce & Mead, 2009), which provides important attachment sites for muscles associated with feeding (Cozzi *et al.*, 2017). Thus, the two parts of the whale orbit have very different functional purposes (feeding vs. echolocation/breathing), and are linked to different modules. Loss of mastication has resulted in reduction of masseter and temporalis muscles, which in turn has reduced the size of attachment sites on the skull, including the zygomatic arch and temporal fossa (Marshall, 2017).

Nasal and vault modules of the dolphin skull

The nasals form their own isolated module, similar in composition to that module in Cheverud (1995), although with a smaller number of landmarks associated with it. In odontocetes, the nasals form the posterior wall of the nasal passage, and are reduced in size, and dorsoventrally thick (Fordyce & Mead, 2009), largely as a consequence of retrograde cranial telescoping and shifting of the external nares posteriorly (Churchill *et al.*, 2018). Beyond the landmarks associated with the nasal bones, this module also includes the intersection of the sutures between the frontals and interparietal, a midline landmark that in *Delphinus* is located adjacent to the nasals, due to retrograde telescoping of the skull. In terrestrial mammals, the nasal forms a module with elements of the rostrum, and is largely associated with feeding (Goswami, 2006a). With telescoping posteriorly displacing the nasals, they no longer are bound to any elements associated with the feeding apparatus (Goswami, 2006a; Parr *et al.*, 2016). They do not appear to possess significant attachment sites for muscles associated with sound production (Heyning, 1989), and so do not group with the landmarks of the face either. It is unclear exactly what functional relationship this module has, but may be associated simply with posterior movement of the external nares and positioning of the air passages.

The final major module recovered in this study is the vault, which includes landmarks associated with the

supraoccipital as well as the basion. In composition, this module is most similar to the vault module of Cheverud (1995), but also includes the intercondyloid notch, associated with the basion module of that study. Goswami (2006a) placed landmarks associated with this module into two distinct modules, one representing the vault and the other representing the basicranium. Parr *et al.* (2016) found landmarks associated with this module as belonging to three distinct modules, one that includes the basicranium and occipital condyles, the olfactory module, and a module that includes the zygomatic and TMJ. In whales, the landmarks found for this module are associated with attachment sites for neck muscles, or otherwise are related to neck mobility. In contrast to many terrestrial mammals, odontocetes have relatively stiff and immobile necks, capable of some varying degree of flexion and rotation, but no extension (Cozzi *et al.*, 2017). This constraint seems to be related to the relative streamlining of the odontocete bauplan and stabilization of the head, enabling high-speed swimming (Buchholtz, 2001).

Asymmetry and cranial modularity

Odontocete skulls possess an unusually high degree of bilateral asymmetry (Ness, 1967). This asymmetry typically takes the form of greater development and expansion of cranial bones on the right side of the skull. The degree of asymmetry is variable across odontocetes, with some clades showing little asymmetry in size and development of cranial bones (e.g. phocoenids and pontoporiids), while in other taxa, bones on different sides of the face may have completely different morphologies, as in kogiids (Ness, 1967; Huggenberger *et al.*, 2017). Within *Delphinus*, the right premaxilla extends farther posteriorly to nearly contact the nasal, whereas these two bones are widely separated on the left side. The right premaxilla is also much broader than the left in the facial region. There are also more subtle differences in the expansion of the maxilla over the frontal dorsally, as well as differences in the shape of the nasals and position of the dorsal infraorbital foramen on each side. Cranial asymmetry is ancient within odontocetes and evolved multiple times (Geisler *et al.*, 2014), including within the Xenorophidae, one of the earliest diverging lineages of odontocete whale (Geisler *et al.*, 2014; Churchill *et al.*, 2016). Some stem cetaceans (i.e. those outside of crown Cetacea, Neoceti) also have subtle asymmetry (Fahlke *et al.*, 2011), although this differs in important ways from that in Odontoceti and is probably not homologous (Gatesy *et al.*, 2013; Fahlke *et al.*, 2015). Why odontocetes possess such varying degrees of cranial asymmetry is not known, but cranial asymmetry probably plays a role in sound production associated with echolocation (Yurick & Gaskin, 1998; Huggenberger *et al.*, 2017), and may also be influenced by differences in the position of the larynx and pharynx, associated with feeding on different-sized prey underwater (Macleod *et al.*, 2007).

Our study suggests that asymmetry plays an important role in the modularity of the *Delphinus* skull, as do other aspects of their cranial evolution, including retrograde telescoping. When we remove asymmetry from their skulls, we find that our novel hypothesis was not supported as strongly as more simple models of modularity. Instead, the terrestrial mammal module hypothesis of Cheverud (1995), based on data from anthropoid primates, was found to best fit our data.

This shift in model support when asymmetry is corrected for in the odontocete skull implies that, in addition to the influence of echolocation and aquatic feeding, cranial asymmetry plays a huge role in the evolution of modularity and integration of the dolphin skull, and appears to drive increased cranial modularity in odontocetes, relative to typical, more symmetrical, mammals. Asymmetry probably influences both echolocation and feeding, which, as discussed above, influences the modularity of the skull. This result suggests that work on examining modularity in other whale taxa with lesser or greater degrees of cranial asymmetry may reveal different results, with taxa with minor or no cranial asymmetry (e.g. *Pontoporia*) perhaps possessing patterns of modularity similar to those of terrestrial mammals. Furthermore, some whale taxa have even more extreme cranial asymmetry. For instance, pygmy and dwarf sperm whales (*Kogia*) not only have some of the most extreme cranial asymmetry of any whale, but also completely lack nasals, possess a distinctive supracranial basin and have an extremely well-developed lacrimal–jugal (Heyning, 1989). These modifications suggest that *Kogia* and other physeteroid whales may have their own unique pattern of modularity, and we may find an unusually high degree of variation in modularity patterns within whales in general, especially taking into account other oddball taxa such as *Monodon* and *Platanista*, and extinct whales such as xenorophids and *Odobenocetops*. Further studies, using larger sample sizes of taxa, and a more diverse set of taxa, should be performed to assess whether the novel module hypothesis recovered in our study applies to all or most odontocetes, and to further test the role of cranial asymmetry in influencing modularity.

ACKNOWLEDGEMENTS

We thank N. Simmons and E. Westwig for access to AMNH collections, and R. Felice for assistance in analyses. Funding was provided by NSF EAR 1349607. We also thank Travis Park, Olivier Lambert and an anonymous reviewer for their thoughtful and useful comments on the paper.

REFERENCES

Adams DC. 2016. Evaluating modularity in morphometric data: challenges with the RV coefficient and a new test measure. *Methods in Ecology and Evolution* **7:** 565–572.

Adams DC, **Otarola-Castillo E. 2013.** Geomorph: an R package for the collection and analysis of geometric morphometric shape data. *Methods in Ecology and Evolution* **4:** 393–399.

Armfield BA, **Zheng Z**, **Bajpai S**, **Vinyard CJ**, **Thewissen JGM. 2013.** Development and evolution of the unique cetacean dentition. *PeerJ* **1:** e24.

Au WWL. 1993. *The sonar of dolphins*. New York: Springer.

Bell CH, **Kemper CM**, **Conran JG. 2002.** Common dolphins *Delphinus delphis* in southern Australia: a morphometric study. *Australian Mammals* **24:** 1–10.

Bloodworth B, **Marshall CD. 2005.** Feeding kinematics of *Kogia* and *Tursiops* (Odontoceti: Cetacea): characterization of suction and ram feeding. *Journal of Experimental Biology* **208:** 3721–3730.

Buchholtz EA. 2001. Vertebral osteology and swimming style in living and fossil whales (Order: Cetacea). *Journal of the Zoological Society of London* **253:** 175–190.

Cheverud JM. 1982. Phenotypic, genetic, and environmental morphological integration in the cranium. *Evolution* **36:** 499–516.

Cheverud JM. 1995. Morphological integration in the saddle-back tamarin (*Saguinus fuscicollis*) cranium. *American Naturalist* **145:** 63–89.

Churchill M, **Geisler JH**, **Beatty BL**, **Goswami A. 2018.** Evolution of cranial telescoping in echolocating whales. *Evolution* **72:** 1092–1108.

Churchill M, **Martinez MR**, **Muizon C**, **Geisler JH**, **Mnieckowski J. 2016.** The origin of high frequency hearing in whales. *Current Biology* **16:** 2144–2149.

Committee on Taxonomy. **2017.** *List of marine mammal species and subspecies*. Yarmouth Port: Society for Marine Mammalogy. Available at: www.marinemammalscience.org.

Cozzi B, **Huggenberger S**, **Oelschläger HA. 2017.** *Anatomy of dolphins: insights into body structure and function*. London: Elsevier.

Cranford TW, **Amundin M**, **Norris KS. 1996.** Functional morphology and homology in the odontocete nasal complex: implications for sound generation. *Journal of Morphology* **228:** 223–285.

Cranford TW, **Elsberry WR**, **Van Bonn WG**, **Jeffress JA**, **Chaplin MS**, **Blackwood DJ**, **Carder DA**, **Kamolnick T**, **Todd MA**, **Ridgway SH. 2011.** Observation and analysis of sonar signal generation in the bottlenose dolphin (*Tursiops truncatus*): evidence for two sonar sources. *Journal of Experimental Marine Biology and Ecology* **407:** 81–96.

Cranford TW, **Krysl P**, **Hildebrand JA. 2008a.** Acoustic pathways revealed: simulated sound transmission and reception in Cuvier's beaked whale (*Ziphius cavirostris*). *Bioinspiration and Biomimetics* **3:** 016001.

Cranford TW, **Mckenna MF**, **Soldevilla MS**, **Wiggins SM**, **Goldbogen JA**, **Shadwick RE**, **Krysl P**, **St. Leger JA**, **Hildebrand JA. 2008b.** Anatomic geometry of sound transmission and reception in Cuvier's beaked whale (*Ziphius cavirostris*). *The Anatomical Record* **291:** 353–378.

Cranford TW, **Trijoulet V**, **Smith CR**, **Krysl P. 2014.** Validation of a vibroacoustic finite element model using bottlenose dolphin simulations: the dolphin biosonar beam is focused in stages. *Bioacoustics* **23:** 161–194.

Cunha H, **Loizaga de Castro R**, **Secchi ER**, **Crespo EA**, **Lailson-Brito J**, **Azevedo AF**, **Lazoski C**, **Solé-Cava AM. 2015.** Molecular and morphological differentiation of common dolphins (*Delphinus* sp.) in the Southwestern Atlantic: testing the two species hypothesis in sympatry. *PLoS ONE* **10:** e0140251.

del Castillo DL, **Viglino M**, **Flores DA**, **Cappozzo HL. 2017.** Skull ontogeny and modularity in two species of *Lagenorhynchus*: morphological and ecological implications. *Journal of Morphology* **278:** 203–214.

Deméré TA, **McGowen MR**, **Berta A**, **Gatesy J. 2008.** Morphological and molecular evidence for a stepwise evolutionary transition from teeth to baleen in mysticete whales. *Systematic Biology* **57:** 15–37.

Drake AG, **Klingenberg CP. 2010.** Large-scale diversification of skull shape in domestic dogs: disparity and modularity. *American Naturalist* **175:** 289–301.

Fahlke JM, **Gingerich PD**, **Welsh RC**, **Wood AR. 2011.** Cranial asymmetry in Eocene archaeocete whales and the evolution of directional hearing in water. *Proceedings of the National Academy of Sciences USA* **108:** 14545–14548.

Fahlke JM, **Hampe O. 2015.** Cranial symmetry in baleen whales (Cetacea, Mysticeti) and the occurrence of cranial asymmetry throughout cetacean evolution. *The Science of Nature* **102**:1–16

Fish FE, **Hui CA. 1991.** Dolphin swimming - a review. *Mammalian Review* **21:** 181–195.

Fordyce RE. 1982. Dental anomaly in a fossil squalodont dolphin from New Zealand, and the evolution of polydonty in whales. *New Zealand Journal of Zoology* **9:** 419–426.

Fordyce RE, **Mead JG. 2009.** The therian skull: a lexicon with emphasis on the odontocetes. *Smithsonian Contributions to Zoology* **627:** 1–248.

Fraser FC, **Purves PE. 1960.** Hearing in cetaceans: evolution of the accessory air sacs and the structure and function of the outer and middle ear in recent cetaceans. *Bulletin of the British Museum of Natural History Zoological series* **7:** 1–141.

Galatius A, **Goodall RNP. 2016.** Skull shapes of the Lissodelphininae: radiation, adaptation, and asymmetry. *Journal of Morphology* **277:** 776–785

Galatius A, **Kinze CC**, **Teilmann J. 2012.** Population structure of harbour porpoise in the Baltic region: evidence of separation based on geometric morphometric comparisons. *Journal of the Marine Biological Association of the United Kingdom* **92:** 1669–1676.

Gatesy J, **Geisler JH**, **Chang J**, **Buell C**, **Berta A**, **Meredith R**, **Springer MS**, **McGowen MR. 2013.** A phylogenetic blueprint for a modern whale. *Molecular Phylogenetics and Evolution* **66:** 479–506.

Geisler JH, **Colbert MW**, **Carew JL. 2014.** A new fossil species supports an early origin for toothed whale echolocation. *Nature* **508:** 383–386.

Geisler JH, **Sanders AE. 2003.** Morphological evidence for the phylogeny of Cetacea. *Journal of Mammalian Evolution* **10:** 23–129.

Goswami A. 2006a. Cranial modularity shifts during mammalian evolution. *American Naturalist* **168:** 270–280.

Goswami A. 2006b. Morphological integration in the carnivoran skull. *Evolution* **60:** 169–183.

Goswami A, **Finarelli JA. 2016.** EMMLi: a maximum likelihood approach to the analysis of modularity. *Evolution* **70:** 1622–1637.

Goswami A, **Polly PD. 2010.** Methods for studying morphological integration and modularity. In: Alroy J, Hunt G, eds. *Quantitative methods in paleobiology*. Bethesda: The Paleontological Society, 213–243.

Heyning JE. 1989. Comparative facial anatomy of beaked whales (Ziphiidae) and a systematic revision among the families of extant Odontoceti. *Contributions in Science, Natural History Museum of Los Angeles County* **464:** 1–64.

Heyning JE, **Mead JG. 1990.** Evolution of the nasal anatomy of cetaceans. In: Thomas JA, Kastelein RA, eds. *Sensory abilities of cetaceans*. New York: Springer, 67–79.

Heyning JE, **Perrin WF. 1994.** Evidence for two species of common dolphins (genus *Delphinus*) from the Eastern North Pacific. *Contributions in Science, Natural History Museum of Los Angeles County* **442:** 1–35.

Hocking DP, **Marx FG**, **Park T**, **Fitzgerald EMG**, **Evans AR. 2017.** A behavioral framework for the evolution of feeding in predatory aquatic mammals. *Proceedings of the Royal Society B* **284:** 20162750.

Huggenberger S, **Leidenberger S**, **Oelschläger HA. 2017.** Asymmetry of the nasofacial skull in toothed whales (Odontoceti). *Journal of Zoology* **302:** 15–23.

Kienle SS, **Law CJ**, **Costa DP**, **Berta A**, **Mehta RS. 2017.** Revisiting the behavioural framework of feeding in predatory aquatic mammals. *Proceedings of the Royal Society B* **284:** 20171035.

Legendre P, **Legendre L. 1998.** *Numerical ecology*. Amsterdam: Elsevier Science.

Machado FA, **Zahn TMG**, **Marroig G. 2018.** The evolution of morphological integration in the skull of Carnivora (Mammalia): changes in Canidae lead to increased evolutionary potential of facial traits. *Evolution* **72:** 1399–1419.

Macleod CD, **Reidenberg JS**, **Weller M**, **Santos MB**, **Herman J**, **Goold J**, **Pierce GJ. 2007.** Breaking symmetry: the marine environment, prey size, and the evolution of asymmetry in cetacean skulls. *The Anatomical Record* **290:** 539–545.

Marshall CD. 2017. Feeding morphology. In: Perrin WF, Würsig B, Thewissen JMG, eds. *Encyclopedia of marine mammals,* 3rd edn. London: Elsevier, 406–414.

Mckenna MF, **Cranford TW**, **Pyenson ND**, **Berta A. 2011.** Morphological diversity of the odontocete melon and its implications for acoustic function. *Marine Mammal Science* **28:** 690–713.

Mead JG. 1975. Anatomy of the external nasal passages and facial complex in the Delphinidae (Mammalia: Cetacea). *Smithsonian Contributions to Zoology* **207:** 1–72.

Miller GSJ. 1923. The telescoping of the cetacean skull. *Smithsonian Miscellaneous Collections* **76:** 1–71.

Mitteroecker P, **Bookstein F. 2008.** The evolutionary role of modularity and integration in the hominoid cranium. *Evolution* **62:** 943–958.

Natoli A, **Cañadas A**, **Peddemors VM**, **Aguilar A**, **Vaquero C**, **Fernández-Piqueras P**, **Hoelzel AR. 2006.** Phylogeography and alpha taxonomy of the common dolphin (*Delphinus* sp.). *Journal of Evolutionary Biology* **19:** 943–954.

Ness AR. 1967. A measure of asymmetry of the skulls of odontocete whales. *Journal of Zoology* **153:** 209–221.

Norris KS. 1964. Some problems of echolocation in cetaceans. In: Tavolga W, ed. *Marine bio-acoustics*. New York: Pergamon Press, 317–336.

Olson EC, **Miller RL. 1958.** *Morphological integration*. Chicago: University of Chicago Press.

Parr WCH, **Wilson LAB**, **Wroe S**, **Colman NJ**, **Crowther MS**, **Letnic M. 2016.** Cranial shape and modularity of hybridization in dingoes and dogs; Hybridization does not spell the end for native morphology. *Evolutionary Biology* **43:** 171–187.

Peredo CM, **Peredo JS**, **Pyenson N. 2018.** Convergence on dental simplification in the evolution of whales. *Paleobiology* **44:** 434–443.

Pigliucci M, **Preston K. 2004.** *Phenotypic integration*. Oxford: Oxford University Press.

Porto A, **Shirai LT**, **Bandoni de Oliveira F**, **Marroig G. 2013.** Size variation, growth strategies, and the evolution of modularity in the mammalian skull. *Evolution* **67:** 3305–3322.

Racicot RA, **Berta A. 2013.** Comparative morphology of porpoise (Cetacea: Phocoenidae) pterygoid sinuses: phylogenetic and functional implications. *Journal of Morphology* **274:** 49–62.

Rommel SA, **Costidis AM**, **Fernández A**, **Jespson PD**, **Pabst DA**, **McLellan WA**, **Houser DS**, **Cranford TW**, **Van Helden AL**, **Allen DM**, **Barros NB. 2006.** Elements of beaked whale anatomy and diving physiology and some hypothetical causes of sonar-related stranding. *Journal of Cetacean Research and Management* **7:** 189–209.

Santana SE, **Lofgren SE. 2013.** Does nasal echolocation influence the modularity of the mammal skull? *Journal of Evolutionary Biology* **26:** 2520–2526.

Schlager S. 2017. Morpho and Rvcg - shape analysis in R. In: Zheng G, Li S, Szekely G, eds. *Statistical shape and deformation analysis*. Cambridge: Academic Press, 217–256.

Segura-García I, **Gallo JP**, **Chivers S**, **Díaz-Gamboa R**, **Hoelzel AR. 2016.** Post-glacial habitat release and incipient speciation in the genus *Delphinus*. *Heredity* **117:** 400–407.

Shirai LT, **Marroig G. 2010.** Skull modularity in Neotropical marsupials and monkeys: size variation and evolutionary constraint and flexibility. *Journal of Experimental Zoology* **314B:** 663–683.

Suzuki R, **Shimodaira H. 2006.** Pvclust: an R package for assessing the uncertainty in hierarchical clustering. *Bioinformatics* **22:** 1540–1542.

Werth AJ. 2000. Feeding in marine mammals. In: Schwenk K, ed. *Feeding: form, function, and evolution in tetrapod vertebrates*. San Diego: Academic Press, 487–526.

Werth AJ. 2006. Mandibular and dental variation and the evolution of suction feeding in Odontoceti. *Journal of Mammalogy* **87:** 579–588.

Whitmore FC, **Sanders AE. 1976.** Review of Oligocene Cetacea. *Systematic Zoology* **25:** 304–320.

Wiley DF, **Amenta N**, **Alcanatara DA**, **Ghosh D**, **Kil YJ**, **Delson E**, **Harcourt-Smith W**, **Rohlf FJ**, **St JK**, **Hamann B. 2005.** Evolutionary morphing. In *Proceedings of IEEE Visualization 2005 (VIS'05)*. 431–438.

Yurick DB, **Gaskin DE. 1998.** Asymmetry in the skull of the harbour porpoise *Phocoena phocoena* (L.) and its relationship to sound production and echolocation. *Canadian Journal of Zoology* **66:** 399–402.

Zelditch ML, **Wood A**, **Swiderski D. 2009.** Building developmental integration into functional systems: function-induced integration of mandibular shape. *Evolutionary Biology* **36:** 71–87.

SUPPORTING INFORMATION

Additional Supporting Information may be found in the online version of this article at the publisher's web-site:

Appendix S1. List of cranial landmarks used in this study, with description and module assignments.
Appendix S2. Output of EMMLi maximum likelihood model selection model analyses.